DEPOSITION OF CHARGED AEROSOL IN RECONSTRUCTED HUMAN AIRWAY

Diew Koolpiruck, Simant Prakoonwit,
and Wemadeva Balachandran

Department of systems engineering
Brunel University
Uxbridge, Midlesex, UB8-3PH, UK
phone: (1) 408-779-7774; fax: (1) 408-779-3638
e-mail: empgddk@ brunel.ac.uk

The transport and deposition of charge aerosol in a steady-state airflow in reconstructed human airways has been studied. The three-dimensional (3D) geometrical model was reconstructed from a set of CT images. The velocity flow field defined as Laminar flow was evaluated using the Finite Volume Method. Based on Lagrangian dynamic approach, the particle trajectories driven by various forces are governed by Newton's second law. It is assumed that the particle cloud is a dilute dispersed phase flow and has no influence on the fluid motion and there is no effect of humidity on charge particles. This study considers both of the space charge and image charge forces. The Particle-Mesh technique is selected to solve the space charge force, because it reduces the complexity of computation due to a large number of charged particles in simulation. The result shows that the effect of electrostatic mechanism improved the particle deposition related to the number of particles and the charge values.

1. Introduction

There are a significant numbers of numerical studies of aerosol transport and deposition in human airways. They usually modeled the particle transport based on Lagrangain dynamic model in term of motion equations using Newton's Law. The particle's motion equation requires the local airflow velocity, which are often obtained using the Computational Fluid Dynamic (CFD) software. In extrathoracic region, Martonen et. al.[1], and Zhang et. al.[2] have studied three-dimensional simulations of aerosol particle transport and deposition in realistic oral-pharyngeal reconstructed from cast model. For tracheobronchial region, many numerical studies were based on single and double bifurcation models using lung morphometric model. Comer et. al. [3][4] investigated particle deposition in a symmetric double-bifurcation airway. The resulting deposition patterns, particle distribution, trajectories and time evolution were analyzed and compared with experiment data. Later, Zhang et. al.[5] extended the numerical study for a triple bifurcation model with a cyclic inhalation pattern. In alveolar region, the model is different from other respiratory parts. Darquenne [6] simulated the particle deposition with two-dimensional six generations representing human acinus. Therefore, the 3D mesh of model and CFD computation requires a significant memory capacity and processor resource. This limitation affects the numerical study linked with only some part of airway model, i.e., extrathoracic region or some sequences of bifurcation.

In recent studies the method used to create the 3D human airway structure can be divided into 2 groups: the 3D model based on morphological data, and the 3D model based on the image dataset. The first group usually generated models using the knowledge of human lung morphology. Spencer et. al.[7] proposed the human airway network using data-driven and surface modeling techniques. However, this model has a total shape of airway network different from the realistic lung. Kitaoka et. al.[8] introduced a 3D model of the human airway model to tracheobronchial region generated by a deterministic algorithm that incorporates duct branching and space division. The algorithm yields realistic tree structures with morphometric characteristic. Tawhai et. al [9] presented a more accurate 3D model implemented by a 3D tree-growing algorithm for generation of a host-shape dependent airway model. The host-shape of lung represented by a surface mesh derived from magnetic resonance imaging (MRI) data. The generation algorithm produces a conducting airway model with branching characteristic close to the measured data. For the second group, the 3D lung models are reconstructed directly from the scan-image dataset of a patient using imaging visualization techniques. However, the imaging technique practically can be extracted deeply into tracheobronchial region, but these image data are not applicable for alveolus region. The advantage of this model can be applied for any respiratory patient, whose airways differ from a healthy person. For an example, Fetita and Pretuex [10] presented the 3D reconstruction of human bronchial tree from volumetric data acquired by using a high resolution computerized tomography (HRCT) system. Then, they presented the technique for model synthesis for bronchial tree [11].

The effects of electrostatic forces may have significant role in increasing the deposition efficiency in which they have adequate charge levels. Generally, the deposition of charge particles for inhaler application is governed by the combination of space charge and image charge force. The theoretically studies of charge on the deposition of charge particle within respiratory system also had been studied by Yu [12][13]. Balachandran et al. [14] developed a computer model accounting gravitational, Brownian diffusion, inertial impaction and electrostatic forces (both the space charge force and the image charge force). This model accounted only for the inhalation cycles. The results showed that the particle with higher charge tend to deposit in upper region of the respiratory tract, while the particle with negligible degree of charge deposit preferentially in the lower region of respiratory tract or in the alveolar sacs. Bailey et al.[15] presented how electric charge on inhaled particles may increase particle retention in lung with complete inhalation and exhalation cycles. They suggested that electrostatic charge on particle would have no significant effect if the large particles were manipulated. The clinical experiments with charged aerosol deposition in humans had been studied by Melandri et al. [16]. it was shown that charged particles significantly change the deposition pattern in lung.

This numerical study is proposed to extend the understanding of the effect of electrostatic forces (space charge and image charge forces) for sub-micron particles on lung deposition based on reconstructed lung model. The objectives are to illustrate how charge inhaled particle transport varying with time, and how inhaled charged particles may increase the deposition in lung.

2. Theory

2.1 Reconstructed airways model

The 3D reconstructed human airway model generated from image data using imaging techniques usually can be represented by surface representations. These surface meshes are used to build finite element mesh of the whole volumetric model required for CFD software. The image dataset can be acquired using Computed Tomography (CT), Magnetic Resonance Images (MRI), and a High-Resolution Computerized Tomography (HRCT) system. The details reconstruction techniques can be found in [17],[18],[19], and [20].The fundamental steps of reconstruction process can be briefly summarized:

1) *Image enhancement.* This process purpose to improve the quality of image due, such as noise filtering. There are 3 groups of enhancement methods: histogram operation, spatial filtering and frequency filtering.

2) *Image registration*. In case of the integration of information gained from different modalities and acquired from the same anatomical structure, image registration is required the integration process to bring the modalities involved into spatial alignment.
3) *Image segmentation.* The interested region are specified and isolated from the image by segmentation techniques. There are three general segmentation methods including manual, automatic and semiautomatic. There are various techniques purposed for segmentation.
4) *Surface extraction.* This step aims to extract the contour (edge), which defined the surface of structure obtained from segmentation process. Marching cubes algorithm is the popular algorithm implemented for extracting these isosurfaces.
5) *Surface simplification.* After isosurfaces are extracted from segmentation data, it makes possible to generate a large numbers of polygons. Simplification has become important for reducing a numbers of polygons.

2.2 Transport equation

The particle cloud in this study is assumed as a dilute disperse phase, hence it can be assumed that there is no effect of particle to airflow. The steady-state airflow is modelled as a steady laminar incompressible flow. The Lagrangain representation of the dispersed-phase motion is described at a single point moving at its own dependent velocity. The individual particle trajectory can be computed by integrating the force balance that equates the particle inertia with acting on the particle. Various forces acting on a particle are combination of drag, lift, fluid stress gradients, basset history term, wall interaction, and electrostatic forces (see details in [21]). For sub-micron particles, a form of Stoke's drag law is available with a very small response time reaching the terminal velocity. The momentum equation of particle can be simplified in term of particle mobility and the total acting forces on particle.

$$\mathbf{v}_p = \mathbf{v} + B(\sum \mathbf{F}_k) \tag{1}$$

Here, $\mathbf{v}_p$ is the particle's velocity, $\mathbf{v}$ is an airflow velocity, B is particle mobility, and $\mathbf{F}_k$ is the summation of k forces.

2.3 Electrostatic force computation

Based on Lagragian approach, the trajectories of particles could be computed independently, because there is no interacting forces among particles. The electrostatic forces for charged particles must be included in the interacting forces among particles must be considered. Thus the particle trajectories could not be computed independently. The main electrostatic forces for inhaler aerosol application consist of the space charge force the image charge force.

For space charge computation, some techniques are required to reduce the complexity due to a large number of particles. The charge on any particles can be approximately represented as the continuous variables named as the charge density (ρ_q). In the continuous domain, the electrical potential can be represented by Poison's equation, which is a function of the continuous charge density. The potential equation (Poison's equation) can be solved within the same mesh structure model using Finite Volume Method (FVM) or Finite Element Method (FEM). However, these techniques are more complex than Finite Difference Method (FDM). In this study, Particle Mesh technique with Finite Difference Method is chosen, therefore it FFT can be used for solving the potential equation and reduce complexity to $O(n_p+n_g \log n_g)$. In addition, the computing speed may improves by Hardware-based 3D-FFT solver. The disadvantage of this technique is that it requires a uniform mesh. Thus, the hexahedral mesh is added into the software for this purpose.

The image charge force requires the shortest distance between wall and particle. It must search the nearest triangular wall surface to any particle. Therefore there are a large a mount of particles, the nearest distance can be calculated based on mesh approach. These distance vectors are fitted into the mesh represent as a continuous variable. The minimum distance to wall can be interpolated from these vectors on mesh. More details both of the space charge and image charge force computations can be found in [22],[23].

3. Numerical Method and Software Implementation

A 3D human airway model was generated from CT male-cadaver dataset obtained from U.S. National Library of medicine (The visible human project). The image dataset have 512x512 pixels (0.9375x0.9375 mm^2/pixel), 12 bits grey tone resolution at 1 mm. interval. The process of image segmentation, surface extraction and surface simplification are implemented using a commercial software Mimics (Materialise Inc.). This study scopes only in Right Upper part of reconstructed model shown in Fig. 3, because the limitation of computation resources.

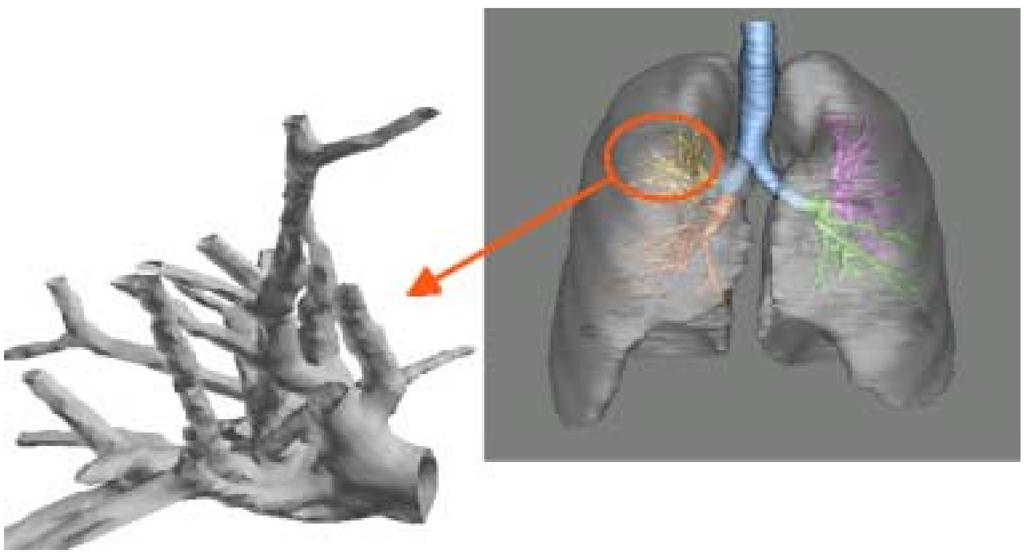

Figure 3. A right-upper reconstructed lung region which is reconstructed from the VHD image dataset.

The simulation program is composed of 2 mesh topologies: tetrahedral and hexahedral meshes. Due to the irregular shape of airway model, the unstructured mesh is suitable for volumetric mesh, generally represented by tetrahedral topology. The complexity of mesh generation relates to the complexity of geometry. GAMBIT software (Fluent Inc.) is chosen for initialising mesh and incorporated with TGRID software (Fluent Inc.) for smoothing, clean-up and refinement. The node pattern for tetrahedral is defined by 4 node at the corner of tetrahedral mesh. For hexahedral mesh, it is auxiliary mesh proposed for PM method for representing charge density of particle cloud. It has a uniform mesh size and independent from tetrahedral.

The solutions of continuity and momentum equation were carried out using FLUENT software (Fluent Inc.), which was developed based on Finite Volume Method. The numerical scheme uses Segregated solver. For discretization schemes, the pressure standard scheme was chosen for pressure variable with relaxation factor of 0.3. The second-order windup differencing scheme was selected for momentum variables with the relaxation factor of 0.7. Pressure-Velocity coupling was employed by a SIMPLEC algorithm. The solutions of these variables were continuously solved until the mass residual of all variables less than 0.001. In this study, FLUENT was run on the workstation Sun-Fire280, with 900 MHz UltraSPARC III processores, and 4096 Mbytes RAM.

The user developed software was implemented for calculating the space charge forces and the image charge force, and integrating of particle's motion equations. The mesh of the model was exported from FLUENT and imported into the developed software. The software checked the imported mesh using mesh information, i.e., the grid size data (numbers of node, face, and cells), the volume data (the minimum, maximum and total cell-volume), and the boundary data. In addition, the velocity of airflow was imported into node data for representing the local flow field. In any particle position, the velocity vector is interpolated using the linear interpolation at nodes of the current cell. The integration of motion equation was employed using Leap-frog algorithm with a constant time step. The details of interpolation calculation can be found in [24]. The sequence of computation in any loop can be concluded as following:

1. Track the current tetrahedral and hexahedral cells and check particle trapped-status.
2. Run PM calculation routine discussed in section B for solving the space charge field.
3. Calculate all forces acting on particles.
4. Solve the particle's motion equation.
5. Update the new particle position and save particle's trajectory data.

4. Results and discussion

4.1 Validation space charge computation

The developed software was set up for validating the computation of space charge effect in a Weibel's model of generation 9. The particle cloud has a uniformly unipolar-charged value of 500e and a uniform particle's position distribution along the whole tube. Using the same assumption in [12]. With mesh size of 128x128x128, the simulation results of depositions agree with the analytical prediction shown in Figure 1. However, the simulation results deviated for the analytical results at the high concentration because the short-range distance force term has more predominant effect. In PM method, the mesh size affects the accuracy of computation. Figure 2 shows the particle deposition against concentration with various mesh size. It shown that the mesh size 64x64x64 has the worse results than the higher mesh size. The higher mesh size is more accurate than the lower mesh size, but it requires more computation time and memory resources. Thus, the mesh size should be selected for optimizing both of accuracy and computing speed.

For the image force computation, the simulation deposition of a uniform charge distribution and a uniform particle's position along the tube due to the image force and analytical agrees with the analytical calculation. It deviated slightly at the low concentration. Using the mesh-based interpolation for the nearest distance between wall and particle, there is an error from mesh interpolation and the discretization of triangular surface representing the wall. The discretization of near-wall distance depends on the number of meshes representing the model. Within a tube generation 3 (0.003 m. in diameter) represented by 64,478 tetrahedral meshes and the number of 227,700 particles in the simulation, the absolute average error is 1.77e-6m. with a standard deviation of 1.72e-5.

4.2 Deposition of charged deposition in the reconstructed airways

The reconstructed model was meshed into 1,404,767 tetrahedral meshes for computing airflow variables. This study modelled the airflow as steady-state laminar flow using the conditions of an inlet Reynolds number of 1,745 with flat velocity profile. No-slip conditions are defined to wall boundaries. The results of airflow velocity carried out by FLUENT

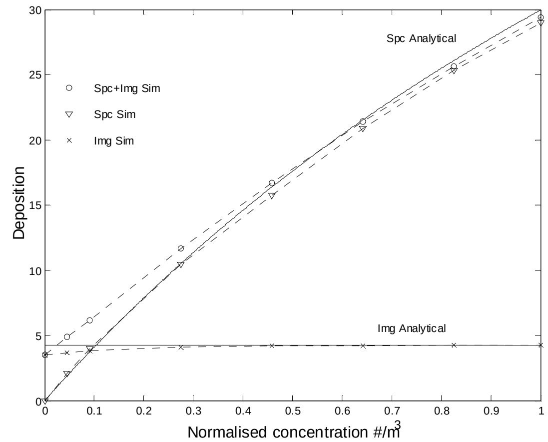

Figure 1. A comparison of particle deposition between the analytical prediction and computer simulation for sedentary breathing with a uniform charge distribution and a uniform particle position.

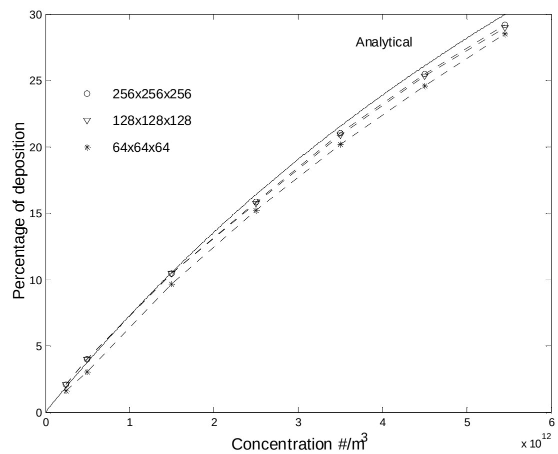

Figure 2. A comparison of particle deposition of various mesh sizes for sedentary breathing with a uniform charge distribution and a uniform particle position.

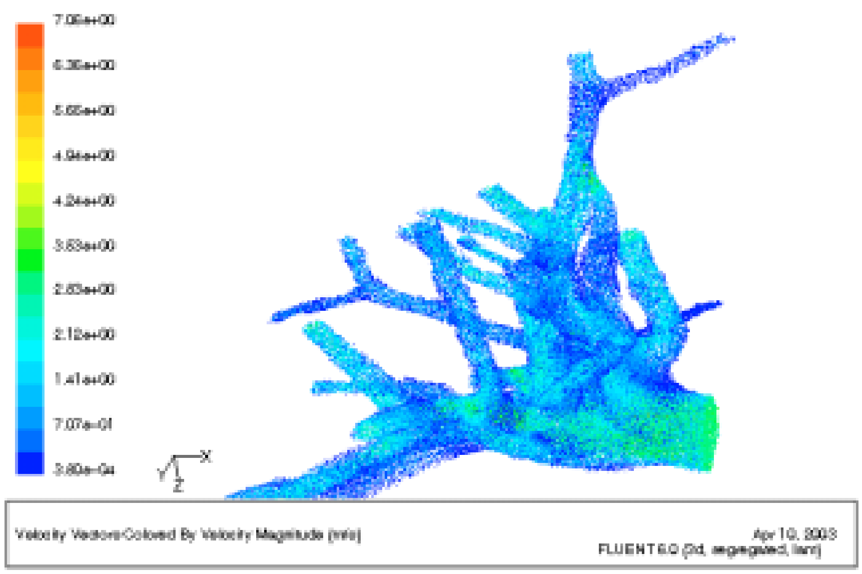

Figure 3. Vector display of velocity magnitude in the reconstructed model with Reynold number of 1750 at inlet.

software are shown in Figure 3 using vector plot. The velocity magnitudes decrease from the main inlet to daughter branches. For the electrostatic forces computation, the inlet particle cloud is assumed as the uniform distributions of positions and charge values. It assumes that there is no effect of humidity on charge particles. The particles are modelled as spherical particles with a uniform diameter of 0.5 μm. The initial particle cloud is cylindrical in shape at main inlet branch with an approximately volume of 3.486×10^7 m^3. The simulations are carried out for charged value of 250e and 500e with the total number of 2,000,000 particles. Figure 4 shows the some iso-surface and coordinate surfaces of electrical field for a uniform charge value of 500e at the initial step. The electrical field is strong near particle cloud and rapidly decrease when position is far away.

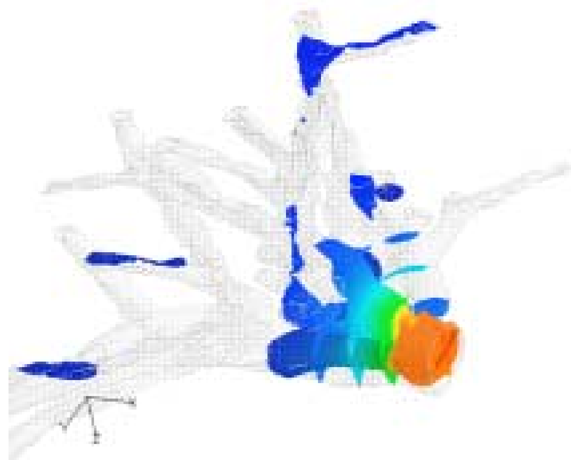

Figure 4 Display some iso-surface and coordinate surfaces of the magnitude of electrical fields in the reconstructed model after releasing the particles.

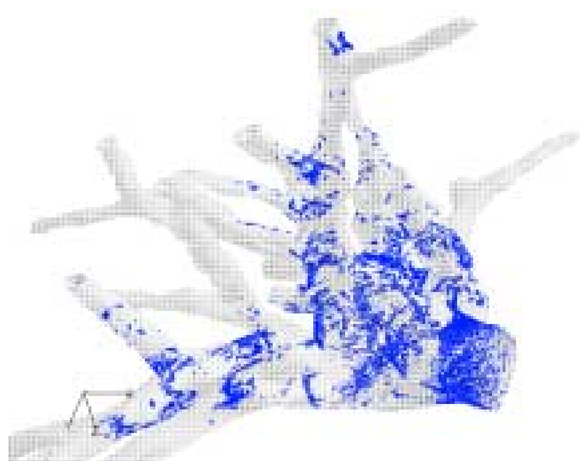

Figure 5 Display the deposition of charge particle on the wall of reconstructed model with a uniform charge distribution of 500e.

The simulation results of particle deposition of various charge values in the model are shown in Table 1. The deposition of uncharged particle is very small because impaction is extremely small for the sub-micron particles. As the charge per particle increase, the electrostatic forces become predominant in the upper part of respiratory tract. In addition, the simulation enables to investigate the local deposition pattern as shown in figure 5.

Table 1 Comparison the percentage deposition with various charge values

	Uncharged	250e	500e
Deposition percentage	<0.5%	11.5%	22.3%

5. Conclusion

Simulation of particle deposition in reconstructed human airways incorporating the effect of space charge and image charge for sub-micron particle has been developed. The simulation results indicate that the inherent charge carried by aerosol particles have a significant effect on the deposition in the upper respiratory tract. This simulation also enables to investigate the local deposition pattern.

It can be concluded that by controlling the charge of aerosol particles, the deposition in the upper airways can be increased significantly. In addition, the reconstructed airway model enables to extend the study for respiratory patients who have different airway morphology from that of healthy person. Future work will include various distributions of particle sizes and charge values.

References

[1] Martonen T B, Zhang Z, Yue G and Musante C J 2002 *J. Aerosol Sci.* **33** 1095-1110.
[2] Zhang Z, Kleinstreuer C and Kim C S 2002 *J. Aerosol Sci.* **33** 1635-1652.
[3] Comer J K, Kleinstreuer C, Hyun C and Zhang Z 2001 *ASME:J. Fluid Mech.* **435** 25-54.
[4] Comer J K, Kleinstreuer C, Hyun C and Zhang Z 2001 *ASME:J. Fluid Mech.* **435** 55-80.
[5] Zhang Z, Kleinstreuer C. and Kim C S 2002 *J.Aerosol Sci.* **33** 257-281.
[6] Darquenne C 2002 *J. Aerosol Sci.* **33** 1261-1278.
[7] Spencer R M, Schroeter R M and Martonen T B 2001 *Comp. Bio.& Med.* **31** 499-511.
[8] Kitaoka H, Takaki R and Suki B 1999 J. *Appl. Physio.* **87** 2207-2217
[9] Tawhai M H, Pullan A J and Hunter P J 2000 *Annals. Bio. Eng.* **28** 793-802.
[10] Feltta C, Preteux F 1999 *Proceedings SPIE Conference on Nonlinear Image Processing X, IS&T/SPIE's Electronic Imaging '99, San Jose, CA*, 3646, 281-295.
[11] Feltta C, Preteux F 2001 *Proceedings World Multiconference on Systemics, Cybernetics and Informatics, Orlando, FL*, 111-116.
[12] Yu C P 1977 *J. Aerosol Sci.* **8** 237-241.
[13] Yu C P 1985 *Ann. Occup. Hygiene* **29** 219-227.
[14] Balachandran W, Machowski E, Gaura E and Hudson C 1997 *J. Electrostatics* **40&41** 579-584.
[15] Bailey A G, Hashish A H and Willims T J 1998 *J. Electrostatics* **44** 3-10.
[16] Melandri C, Prodi V, Tarroni G, Formignani M, Dezaiacomo T, Bompane G F and Maestri G 1977 *Inhalation Particels IV* 193-201.
[17] Cebral J R and Lohner R. 1999 *Proc. 8th International Meshing Roundtable*, South Lake Tahoe, October 10-13, California.
[18] Cebral, J.R., and Lohner, R 2000., *Proc. ICMMB-11*, April 2-5, Hawaii.
[19] Bankman I H 2000 Handbook of medical imaging: Processing and Analysis, Academic Press.
[20] Robb R A 2000, Biomedical Imaging, Visualization and Analysis, John Wiley&Son.
[21] Loth E 2000, Progress in Energy and Combustion Science. **26** 161-223.
[22] Koolpiruck D, Prakoonwit S and Balachandran W 2003 *ESA&IEEE Conference, June 24-27, Arkansaw.*
[23] Hockney R W, and Eastwood J W 1988 *Computer Simulation Using Particles* (Institute of Physics Publishing).
[24] Kwon Y W, and Bang H C, 2000 *The finite element method using MATLAB* (CRC Press).